

## 6. *IN SITU* PERMEABILITY AND PORE-PRESSURE MEASUREMENTS NEAR THE MID-ATLANTIC RIDGE, DEEP SEA DRILLING PROJECT HOLE 395A<sup>1</sup>

Stephen H. Hickman, U.S. Geological Survey, Menlo Park, California  
Marcus G. Langseth, Lamont-Doherty Geological Observatory  
and  
Joseph F. Svittek, U.S. Geological Survey, Menlo Park, California<sup>2</sup>

### ABSTRACT

The *in situ* permeability and pore pressure of 7.2-Ma-old ocean crust were measured in a 664-m-deep hole (DSDP Hole 395A) near the Mid-Atlantic Ridge. These measurements indicate that the bulk permeability from 583 to 664 m below the sea floor (490–571 m sub-basement) at this site is very low, about 3 to 9 microdarcies, and that the pore pressure in the interval from 180 to 664 m sub-bottom is at least 1.5 b (bars) below the oceanic hydrostat. The measured permeability is so low that it virtually precludes significant hydrothermal convection between 583 and 664 m sub-bottom at Site 395, although depressed downhole temperatures, anomalously low regional heat-flow values, and the subhydrostatic pore pressure indicate that substantial hydrothermal convection is probably occurring at shallower depths. If this low-permeability zone is pervasive (as more recent measurements of low permeabilities at depth in DSDP Hole 504B, near the Costa Rica Rift, suggest), it places strong constraints on the vertical extent of convective transfer in cooling oceanic lithosphere.

### INTRODUCTION

The existence of complex hydrothermal systems near mid-ocean ridges is now well documented. Hydrothermal plumes discharging superheated metal-saturated water have been observed directly near the East Pacific Rise (Speiss et al., 1980), and they indicate extremely energetic convective processes near active oceanic spreading centers. In addition, the conductive heat fluxes observed in young oceanic lithosphere are frequently low, compared with values predicted by oceanic-lithosphere-cooling models utilizing purely conductive heat transfer (Lister, 1972; Sclater et al., 1976; Anderson et al., 1977). This suggests that significant heat is transferred across the seafloor by less energetic hydrothermal convection systems, which persist to considerably greater distances from active oceanic spreading centers.

The transition from convective-plus-conductive heat transfer in young ocean crust to a primarily conductive heat-transfer mechanism in older ocean crust is indicated by the disappearance of this heat-flow anomaly. Anderson and Skilbeck (1981) modeled the ocean crust and overlying sedimentary cover as a two-layer porous medium, and found that the location of this transition depends upon the geometry of the convection cells, the thickness of the sedimentary cover, and the permeabilities of the sedimentary cover and basaltic basement. In order to understand the physical mechanisms by which this transition occurs, the packer experiments conducted at Site 395 during DSDP Leg 78B were designed to mea-

sure directly the *in situ* permeability and pore pressure of the basement near the Mid-Atlantic Ridge.

Anderson and Zoback (1982) conducted a similar suite of packer experiments in DSDP Hole 504B, near the Costa Rica Rift, eastern Pacific Ocean, at a location where heat transfer across the sediment/seawater interface appears to be primarily conductive. In that study they found bulk permeabilities ranging from about 40 md (millidarcies<sup>3</sup>) in the pillow basalts and basaltic flows of the lower 173 m of the hole (320–493 m sub-bottom or 45–218 m sub-basement) to 2–4 md in the altered pillow basalts of the lower 15 m of the hole. They also measured formation pore pressures at the bottom of this hole that were approximately 8 b (bars) subhydrostatic. On the basis of the high crustal permeability and subhydrostatic pore pressure measured at this site, and using a simple numerical convection model, Anderson and Zoback concluded that Hole 504B had probably penetrated an active hydrothermal convection cell in the ocean crust which, prior to drilling, had been hydraulically isolated from the seafloor by a relatively impermeable sedimentary cover. As discussed later in this chapter, however, more recent permeability measurements, made by Anderson et al. (1982) in Hole 504B when it was re-entered and deepened during Leg 83, reveal substantially lower permeabilities of approximately  $2 \times 10^{-5}$  darcy (20 microdarcies) at depths of 530 to 1280 m sub-bottom (250–1000 m sub-basement).

### SITE DESCRIPTION

DSDP Site 395 is on 7.2-Ma-old ocean crust on the west side of the Mid-Atlantic Ridge, south of the Kane Fracture Zone (Fig. 1). The experiments discussed in this

<sup>1</sup> Hyndman, R. D., Salisbury, M. H., et al., *Init. Repts. DSDP, 78B*: Washington (U.S. Govt. Printing Office).

<sup>2</sup> Addresses: (Hickman, present address) Department of Earth, Atmospheric and Planetary Sciences, Massachusetts Institute of Technology, Cambridge, MA 02139; (Svittek) U.S. Geological Survey, 345 Middlefield Road, Menlo Park, CA 94025; (Langseth) Lamont-Doherty Geological Observatory, Columbia University, Palisades, NY 10964.

<sup>3</sup> 1 darcy  $\approx 10^{-2}$  m<sup>2</sup>.

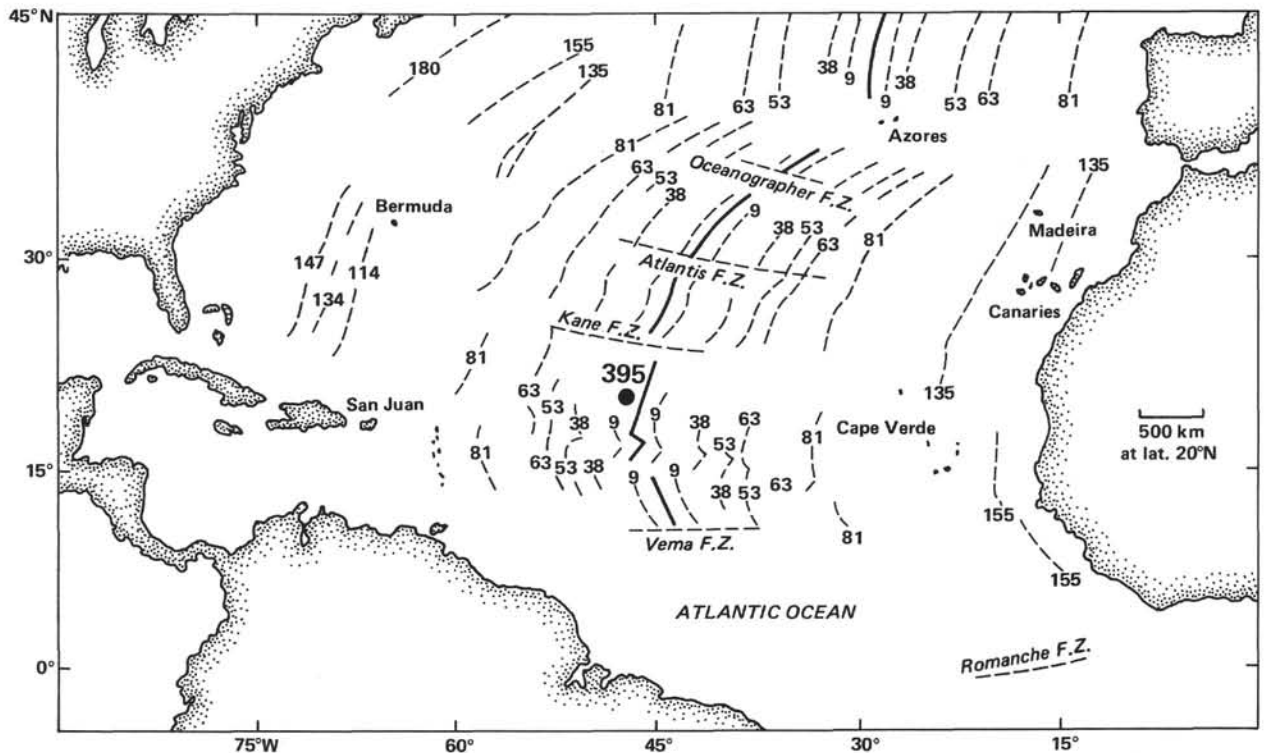


Figure 1. Location of Deep Sea Drilling Project Site 395. Dashed lines with numbers indicate significant magnetic anomalies, with base-met ages given in Ma (from Dmitriev, Heitzler, et al., 1976).

paper were conducted in Hole 395A, the deeper of two holes drilled at this site during Leg 45. Hole 395A was drilled in water approximately 4.5 km deep to a total sub-bottom depth of 664 m, of which the upper 93 m were in sediments and the upper 112 m were cased. It was re-entered during Leg 78B (about five years later) for the purposes of conducting downhole geophysical measurements, collecting drill-hole and formation-water samples for geochemical analysis, and emplacing an experimental downhole seismometer package.

The predominant rock types recovered during the drilling of Hole 395A were phyric and aphyric basaltic pillow lavas, with occasional thin basaltic flows and breccias. In addition, at least one large dolerite intrusion was encountered near the bottom of the hole. The igneous basement in the vicinity of the site is only thinly covered by sediments, which occur largely as isolated pockets in topographic lows. Hole 395A was spudded into one of these sediment ponds, and is surrounded on all sides by high-relief, sediment-free basement (Hussong et al., 1979).

Shallow heat-flow measurements were made in sediment ponds in the vicinity of Site 395 by Hussong et al. (1979) and Purdy et al. (1979). Disregarding one anomalously high heat-flow value of 120 mW/m<sup>2</sup> and another questionable value derived from a highly erratic vertical temperature profile, these eight measurements indicate a mean heat flow of  $33 \pm 9.6$  mW/m<sup>2</sup>. Simple thermal models for oceanic lithosphere cooling solely by conduction predict heat flow as a function of age as  $HF = 480/\sqrt{t}$ , where  $t$  is in millions of years (Parsons and Scla-

ter, 1977). Using this relationship, the heat flow predicted for this site is 180 mW/m<sup>2</sup>, or approximately 5.5 times the average measured value. As pointed out by Purdy et al. (1979), the large difference between the predicted and observed heat flows at this site can best be attributed to the transfer of large quantities of heat into the overlying water column by hydrothermal convection.

#### EQUIPMENT

The inflatable packer used in this experiment (a Lynes International Daring-Drilling-Safety-Test tool) is resettable and operates in two modes. In the first mode (Fig. 2A) the packer is operated using a downhole tool known as a safety go-devil (in this chapter the term "go-devil" refers to any device that is allowed to fall freely down the drill pipe). To operate the packer with this tool, the packer is first lowered to the test depth on the end of the drill string. The safety go-devil is then dropped into the drill string and lands in the packer. When the wellhead pressure is raised about 35 b, the packer inflation check-valve opens and the packer inflates. At a wellhead pressure of about 114 b the shear plug blows through and allows communication between the pump at the wellhead and the hole below the packer. The packer remains inflated against the borehole wall and isolates the open hole below the packer from the annulus. In many cases this "blowing through" of the shear plug will create in the hole below the packer a positive pressure pulse, which can then be analyzed using the slug test method (described herein under "Methods: Permeability Tests") to determine the formation permeability. A pressure transducer at the wellhead and a pressure recorder suspended below the packer record the wellhead and downhole pressures, respectively. A surface flowmeter provides a continuous record of the flow rate for both the slug and steady-state injection tests.

In the second mode (Fig. 2B) a different type of go-devil is used to operate the packer. This device, the sampler go-devil, is designed primarily to collect large-volume water samples from the hole below the packer. In a manner similar to that for the safety go-devil, the sampler go-devil is dropped into the drill string and seats in the packer. When

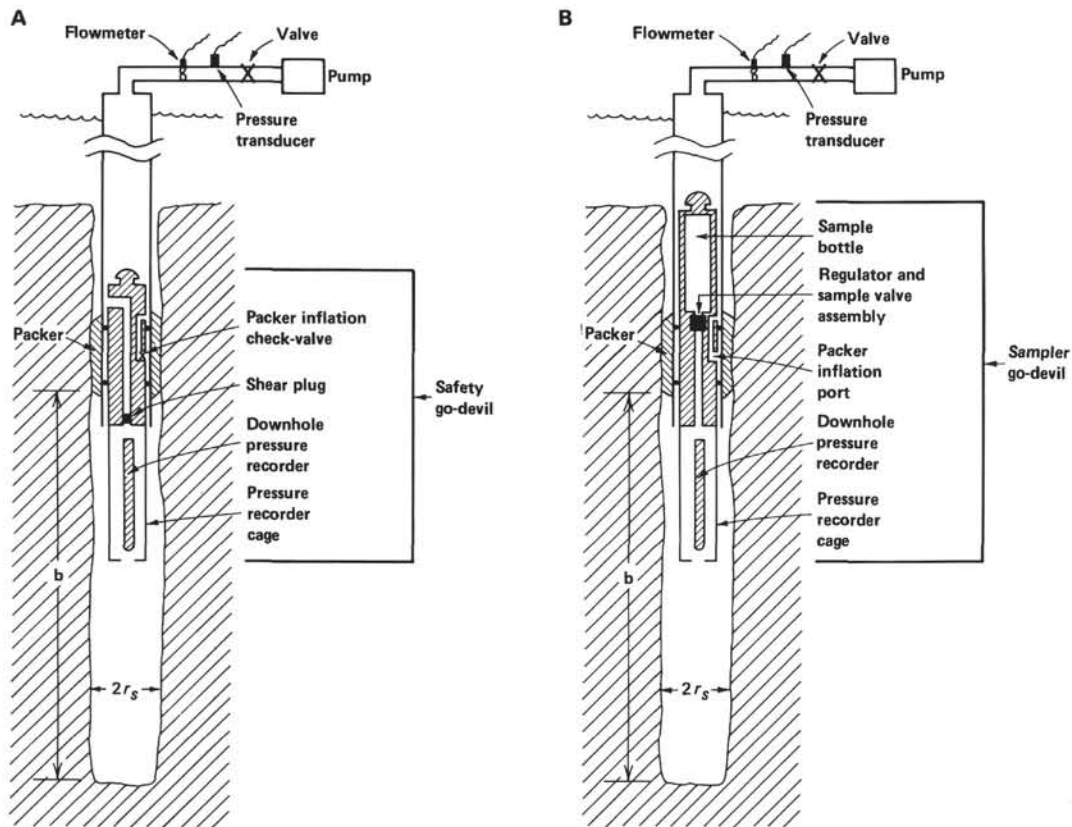


Figure 2. Schematic of packer assembly inflated downhole and shipboard equipment for (A) the safety go-devil operation and (B) the sampler go-devil operation.

the drill-string pressure is raised, the packer inflates. The sample valve then opens at a wellhead pressure of about  $75b$ , allowing for the sudden intake of water from the hole below the packer (which is at hydrostatic pressure) into the sample bottle (which is at atmospheric pressure). If the transmissivity and hole volume below the packer are low enough, this sample collection will create a negative pressure pulse below the packer. The record of this pulse on the downhole pressure recorder can then be analyzed using the slug test method to determine the formation permeability.

Not shown in Figure 2 are the bumper subs—telescoping downhole heave-compensators that are placed in the drill string directly above the packer. These devices expand and contract in response to vertical movements of the ship, and are intended to protect the packer from wave-induced load surges.

## METHODS

### Permeability Tests

As with most *in situ* measurements of permeability, the rock here is assumed to be homogeneous and isotropic. The homogeneity assumption states that, when calculating permeability, fractured crystalline rock can be treated as a uniformly permeable medium. Water is assumed to flow everywhere through the rock surrounding the test wells, instead of through open fractures only. This assumption becomes more valid as the scale of the permeability test increases with respect to the spacing of the fractures, so that effects of flow through individual fractures are essentially averaged. Making this assumption, one can compute the Darcian or equivalent porous-media permeability. In this chapter we designate the permeability thus obtained as the bulk permeability. A thorough justification for applying Darcy's law to fractured rocks has been presented by Parsons (1966).

There are two versions of the slug test. The first, the conventional slug test, is useful in testing high-permeability formations, and is discussed by Cooper et al. (1967) and Papadopoulos et al. (1973). The second version, the modified slug test, is useful in testing low-permeability formations, and is discussed by Bredehoeft and Papadopoulos (1980).

The method used in measuring the *in situ* bulk permeability in Hole 395A was the modified slug test. In this version a single rubber packer on the end of a drill string is used to isolate the lower portion of the hole, called the test interval (interval  $b$  in Figs. 2A and 2B). Once the packer is in place, the drill string is "topped off" with water and sealed with a cap, and the packer is inflated. After a brief period of observation of the system pressure, the system is suddenly pressurized by injecting a small volume of water, or "slug," into the drill string. The sudden increase in pressure,  $H_0$ , thus produced then decays with time as water flows radially outward into the aquifer through the test interval. The solution of this transient-flow problem is given by Cooper et al. (1967) and Bredehoeft and Papadopoulos (1980) as

$$H(t)/H_0 = F(\alpha, \beta) \quad (1)$$

where

$$\alpha = \pi r_s^2 S / V_w C_w \rho_w g \quad (2)$$

$$\beta = \pi T t / V_w C_w \rho_w g \quad (3)$$

The equation relates the excess head  $H(t)$  (in the system at a time  $t$ , following addition of the slug), to the well radius  $r_s$ ; the volume of water  $V_w$ , pressurized in the system during slug injection; the compressibility of water  $C_w$ ; the density of water  $\rho_w$ ; the acceleration due to gravity  $g$ ; and to the transmissivity  $T$  and storage coefficient  $S$  of the test interval. For the tests reported here,  $\rho_w$  was taken as  $1.05 \text{ g/cm}^3$  and  $C_w$  was taken as  $3.96 \times 10^{-11} \text{ cm}^2/\text{dyne}$  and  $4.20 \times 10^{-11} \text{ cm}^2/\text{dyne}$  for the sampler and safety go-devil tests, respectively. The function  $F(\alpha, \beta)$  is given by

$$F(\alpha, \beta) = \frac{8\alpha}{\pi^2} \int_0^{\infty} \frac{\exp(-\beta u^2/\alpha)}{u f(u, \alpha)} du \quad (4)$$

where  $f(u, \alpha) = [uJ_0(u) - 2\alpha J_1(u)]^2 + [uY_0(u) - 2\alpha Y_1(u)]^2$  and  $J_0(u)$ ,  $J_1(u)$ ,  $Y_0(u)$ , and  $Y_1(u)$  are the zero and first-order Bessel functions of

the first and second kind. In this test, the recovery of borehole pressure following a negative pulse is analytically identical to the decay of pressure following a positive pulse, so that  $H_0$  and  $H(t)$  may be either positive or negative. The actual behavior, however, may be different, for reasons to be discussed later.

In analyzing data from the slug test, a plot is made of  $H/H_0$  against  $\log t$ . This plot is superimposed on a type-curve plot of  $F(\alpha, \beta)$  against  $\log \beta$  that was prepared by Cooper et al. (1967) and Papadopoulos et al. (1973) for 10 orders of  $\alpha$  ( $\alpha = 10^{-10}$  to  $10^{-1}$ ). A type-curve that best fits the data is then selected. The values of  $t$  and  $\beta$  at which this fit is achieved are related to the transmissivity of the tested interval by equation 3. The  $\alpha$  value of the type-curve used is related to the storage coefficient of the tested interval by equation 2.

The type curves do not vary rapidly with  $\alpha$  (especially for  $\alpha < 10^{-5}$ ), so significant errors, up to two orders of magnitude, in  $\alpha$  are possible from the matching. Fortunately, a large error in  $\alpha$  results in only a relatively small corresponding error in the determined  $T$ . As pointed out by Papadopoulos et al. (1973), for type-curves in the range  $\alpha < 10^{-5}$ , an error in  $\alpha$  of 2 orders of magnitude would result in an error in  $T$  of less than 30%. The storage coefficient, however, is much more sensitive to variations in  $\alpha$ , and an error in  $\alpha$  of 2 orders of magnitude would result in an equally large error in the determination of  $S$ . For this reason both the conventional and modified slug tests are considered inaccurate indicators of aquifer storage coefficient. The data from Hole 395A fit type-curves with a range of  $\alpha$  from  $10^{-4}$  to  $10^{-5}$ , and the uncertainties in transmissivity, bulk permeability, and storage coefficient that will be shown later correspond to uncertainties in  $\alpha$  of approximately one order of magnitude.

The average bulk permeability,  $K$ , for a given test interval is related to the determined transmissivity by

$$K = cT/b \quad (5)$$

where  $K$  is in darcies,  $b$  is the thickness of the test interval, and  $c$  is a conversion factor given by

$$c = (\mu/g\rho_w) \cdot 1.013 \times 10^8 \quad (6)$$

in which both the dynamic viscosity,  $\mu$ , and  $\rho_w$  are functions of temperature, pressure, and salinity. In this study we have taken  $\mu$  as 1.21 cp (centipoise) and  $\rho_w$  as 1.05 g/cm<sup>3</sup>.

In addition to the modified slug test, we had hoped to conduct a suite of steady-state injection tests at each packer location. In this test, water is pumped into the test interval at a constant flow rate until the borehole pressure stabilizes at some equilibrium value. When three or more flow-rate/borehole-pressure combinations are obtained for a given test interval, this test, in addition to corroborating the bulk permeability obtained from the slug test, provides insight into the sensitivity of aquifer permeability to changes in effective stress, the extent of turbulent flow in the aquifer during testing, and the degree of leakage past the packer. An excellent discussion of the theory and practice of steady-state injection tests may be found in Ziegler (1976).

Steady-state injection tests are not practical, however, for testing intervals of very low transmissivities. We were therefore unable to conduct such a test effectively in conjunction with the one good permeability-testing packer seat obtained near the bottom of the hole.

#### Pore-Pressure Measurement

For the pore-pressure measurement we inflated the packer using the safety go-devil, but kept the drill-string pressure low enough to avoid blowing the shear plug. In this way we were able to shut in the hole at the packer and monitor, with the downhole pressure recorder, the borehole pressure below the packer as it converged toward an equilibrium shut-in pressure (see Apps, Doe, et al., 1979, for a discussion of this technique). The time required to achieve an equilibrium shut-in pressure in such a test depends upon such factors as aquifer transmissivity, geometry, and boundary conditions, aquifer and drill-hole storage coefficients, and the length of time during which water was injected into or withdrawn from the well before shut-in. This test provides a clear upper bound for the near-field pore pressure in cases where the borehole pressure is decreasing during shut-in, and a clear lower bound in cases where the borehole pressure is increasing during shut-in.

Horner's (1951) solution for the borehole pressure in an infinite, isotropic, homogeneous aquifer during shut-in may be used to estimate the initial, or undisturbed pore pressure. His solution predicts a linear relationship between the borehole pressure and  $\log [(T + \Delta t)/\Delta t]$ , where  $\Delta t$  is the elapsed shut-in time following fluid injection or withdrawal for a time period  $T$ . The initial reservoir pressure is then obtained by plotting the borehole pressure on the arithmetic axis against  $(T + \Delta t)/\Delta t$  on the logarithmic axis of semi-log paper and extrapolating to infinite elapsed shut-in time. This solution is not applicable in cases where the reservoir is finite or the reservoir pressure is dynamically maintained (e.g., through thermomechanical processes).

## RESULTS

### Operations

The operational aspects of the packer testing program are outlined in Table 1. Permeability measurements were attempted at depths of 180, 183, and 583 m sub-bottom. Of these, only the two permeability tests at 583 m were successful. The other two tests failed because of destruction of the packer element through hammering of the bumper subs in rough seas. A large-volume water sample was collected at 583 m, and a successful pore-pressure measurement was made at 180 m. Upon discovering the zone of extremely low permeability at the bottom of the hole, we decided to attempt a hydraulic fracturing stress measurement at the 583-m packer depth. Pumping to a downhole pressure of 672 b (the maximum pressure we felt it safe to attain without endangering the packer), we were unfortunately not able to induce a hydraulic fracture. This establishes a lower bound on the breakdown pressure below 583 m in this hole. The breakdown pressure is a function of the greatest and least horizontal principal stresses, the pore pressure near the hole, and the formation tensile strength (Hubbert and Willis, 1957). Since only one of these parameters (the pore pressure) may be estimated with any degree of accuracy, this lower bound is of no use in constraining the magnitudes of the horizontal principal stresses at this site. Nevertheless, even at the maximum

Table 1. Packer-testing operations summary, Hole 395A.

Date	Packer depth (m) <sup>a</sup>	Test	Comments
3/25/81, a.m.	583	Large-volume water sample and permeability test using sampler go-devil.	Both successful
3/25/81, p.m.	583	Permeability test using safety go-devil.	Successful
3/25/81, p.m.	583	<i>In situ</i> stress measurement through hydraulic fracturing.	Not successful; we were unable to induce a hydraulic fracture at wellhead pressure of 152 b (maximum differential pressure we felt it safe to attain without endangering packer element).
3/25/81, p.m.	180	Pore-pressure measurement using safety go-devil.	Successful
3/26/81, a.m.	180	Permeability test using safety go-devil.	Not successful; packer element had torn and failed to remain inflated after blow-through of shear plug.
3/30/81, p.m. 3/31/81, a.m.	183	Permeability test using safety go-devil.	Re-entered hole with new packer element; test not successful; hammering of bumper subs in rough seas tore packer element.

<sup>a</sup> Depth below seafloor. To obtain depth below rig floor, add 4495 m; to obtain depth sub-base-ment, subtract 93 m.

attained pressure of 672 b we had exceeded the calculated magnitude of the overburden stress at 583 m sub-bottom by 55 b. The significance of this in relation to the permeability in the bottom of this hole will be discussed later.

### Permeability Tests

Two modified slug tests were conducted with the packer set at 583 m sub-bottom. The first test took place during use of the sampler go-devil. The negative pressure pulse resulting from the opening of the sampler valve and the first 30 min. of the recovery from that pulse were recorded on the downhole pressure recorder. For the second test we used the positive pressure pulse generated in the test interval when the shear plug blew through on the safety go-devil. Figures 3 and 4 show the downhole pressure records for the sampler go-devil and safety go-devil tests, respectively.

The noise on both records results from the alternating compression and tension placed on the packer and bumper subs during ship heave. Fortunately, this noise is largely symmetrical, and pressure readings from adjacent peaks and troughs during periods of relatively constant noise amplitude were averaged to obtain the smoothed decay curves used in our analysis.

The fit of these data to the slug test type-curves is shown in Figure 5. Owing to the extremely low transmissivity encountered in this test interval, there was sufficient time to record only about 20% of the decay (or recovery) from each pulse. Although both tests were conducted at the same depth, the water-volume term  $V_w$  in equation 3 is much larger for the safety go-devil test than for the sampler go-devil test, and the decay rate is correspondingly much slower.

The transmissivities, bulk permeabilities, and storage coefficients from both tests are as follows:

Test interval (m sub-bottom)	Transmissivity ( $10^{-5}$ cm <sup>2</sup> /s)	Bulk permeability ( $10^{-6}$ darcy)	Storage coefficient
583-664 (sampler go-devil)	$1.82 \pm 0.47$	$2.67 \pm 0.69$	$3.30 \times 10^{-8} \pm 1$
583-664 (safety go-devil)	$6.26 \pm 1.27$	$9.20 \pm 1.87$	$3.17 \times 10^{-8} \pm 1$

The errors shown correspond to an uncertainty in  $\alpha$  of approximately  $\pm$  one order of magnitude.

The discrepancy between the bulk permeabilities indicated by the two tests has two possible explanations. Because of the long decay time involved, small leaks in the drill string may have contributed to the pressure decay during the safety go-devil test, resulting in an erroneously high apparent bulk permeability. The sampler go-devil test, since it is isolated from the drill string, would not be vulnerable to contamination from pipe-joint leaks, and would therefore provide a more accurate measure of the bulk permeability in the bottom of this hole. Alternatively, the discrepancy could be explained with reference to the proven dependence of fractured-rock permeability on effective stress (Kranz et al., 1979; Engelder and Scholz, 1981). The large positive pressure pulse of the safety go-devil test ( $H_0 = +91$  b) would be expected to open fractures and increase the permeability in the vicinity of the hole. The sampler go-devil test with its large negative pressure pulse ( $H_0 = -57$  b) would, however, be expected to close fractures

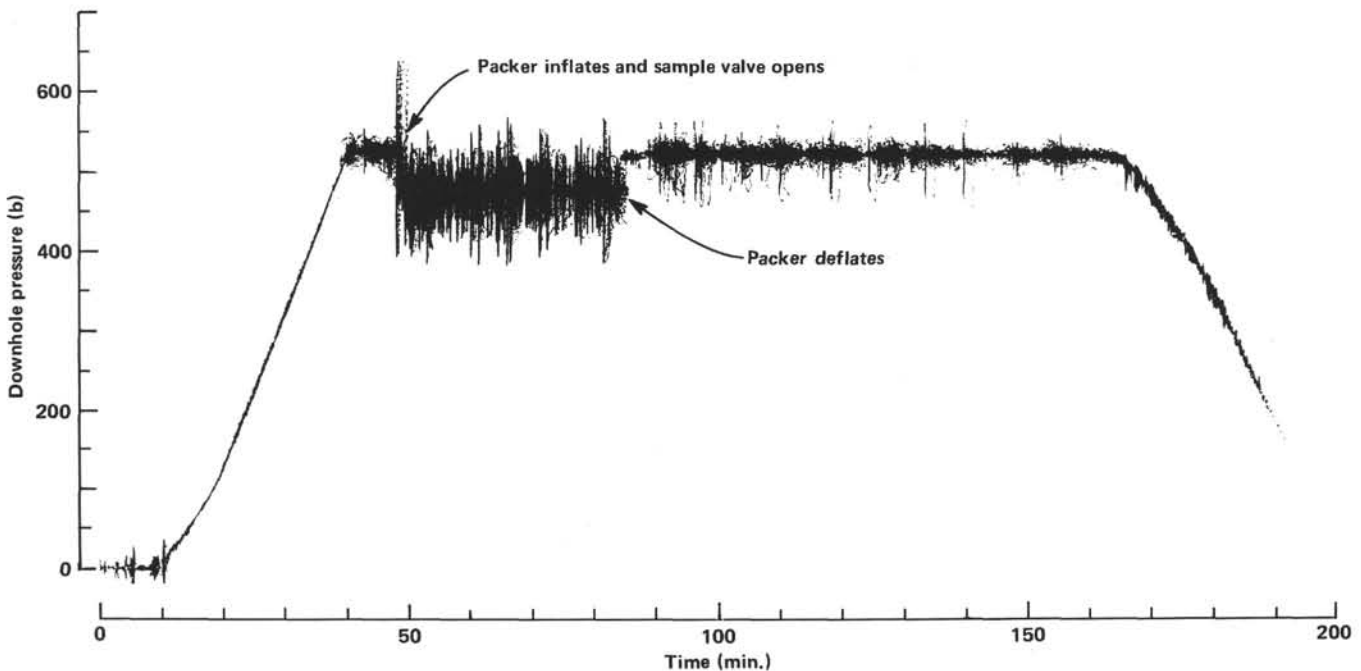


Figure 3. Downhole pressure record from the permeability test conducted at 583 m sub-bottom using the sampler go-devil. Deflation of the packer resulted in sudden equalization of the borehole pressure below the packer and the oceanic hydrostat.

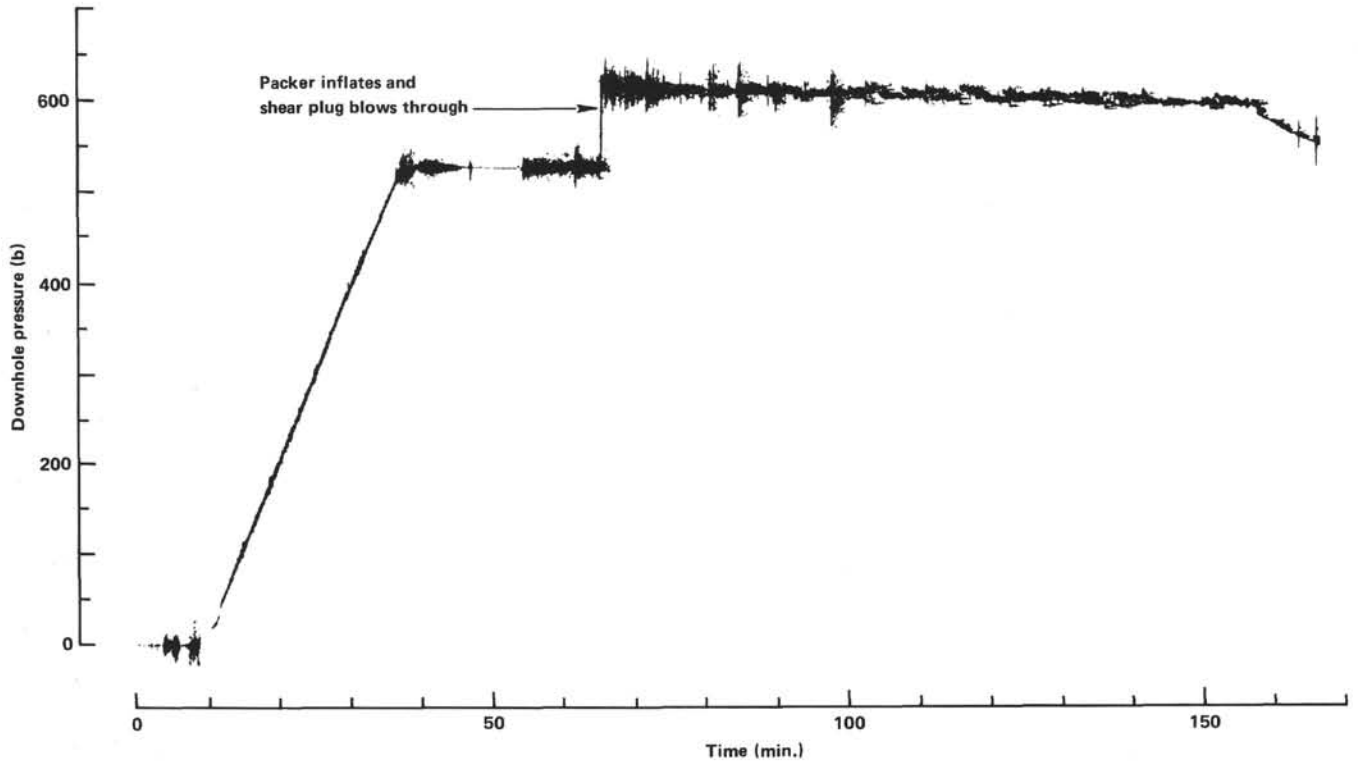


Figure 4. Downhole pressure record from the permeability test conducted at 583 m sub-bottom using the safety go-devil. The increase in pressure decay rate at the end of this test results from bleeding off of fluid at the wellhead before packer deflation.

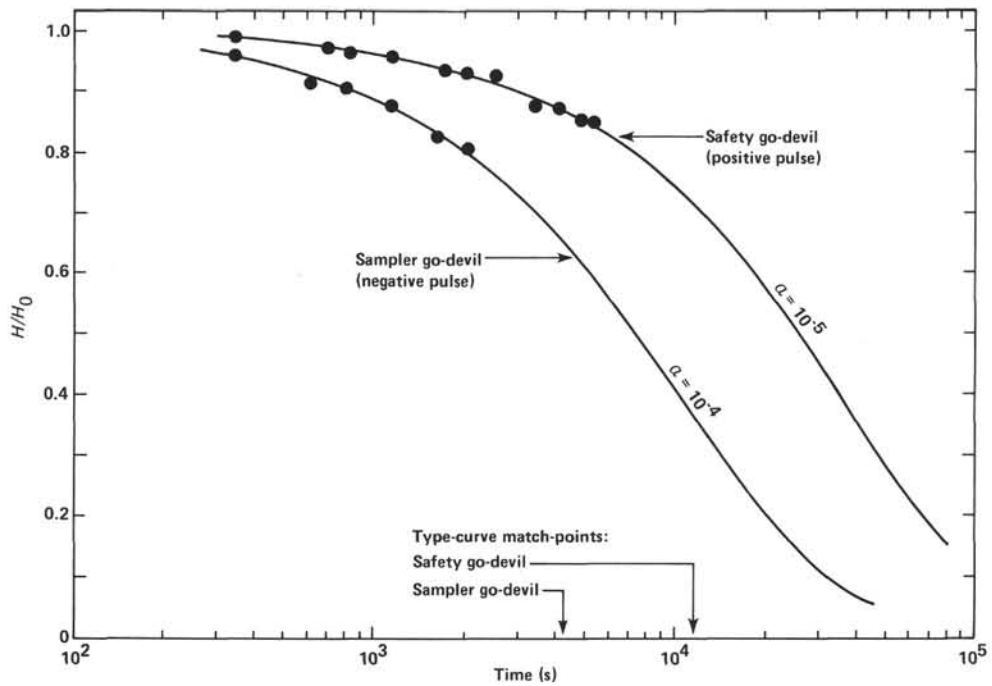


Figure 5. Fit of the data from the two permeability tests at 583 m sub-bottom to the slug test type-curves. The type-curve match-points shown correspond to the time at which  $\beta$  (in equation 3) = 1.

and decrease the permeability in the aquifer surrounding the hole. If these opposite effects do in fact occur, then the actual bulk permeability in the aquifer at the bottom of this well under near-hydrostatic fluid pressures should probably be close to the average of the two values given by these tests, or about  $6 \times 10^{-6}$  darcy. But since we cannot ascertain which is the correct explanation of the discrepancy between permeability test values, all we can say with certainty is that the bulk permeability at the bottom of this hole is between approximately 2.7 and 9.2 microdarcies.

When Hole 395A was re-entered at the beginning of Leg 78B, the apparent open-hole depth (as measured during the various logging runs conducted on this leg) had decreased from the original drilled depth of 664 m to only 609 m (i.e., from 5159 to 5104 m below the rig floor). In our calculations, however, we assume that the hole is still hydraulically open to 664 m sub-bottom. This requires that the hydraulic resistance of whatever material may be blocking the hole below 609 m be negligible for the extremely low borehole flow rates encountered during these slug tests. This seems to be a reasonable assumption, given the slow decay rates observed. But even if we were to assume that the hole was hydraulically open just to 609 m, this would change only the safety go-devil results, since the test-interval thickness terms in equation 3 (as contained in the  $V_w$  term) and equation 5 cancel out when computing bulk permeability from the sampler go-devil test.

At this point it seems pertinent to raise the question of possible contamination of the bottom of this hole by cement and the influence this may have had upon the measured permeability values. When Hole 395A was originally drilled, considerable torquing and hole-stability problems were encountered below a dolerite unit starting at about 608 m sub-bottom. After reaching a total sub-bottom depth of 664 m, the bit was pulled back to 636 m and an attempt was made to stabilize the hole by injecting about 20 barrels (3.18 m<sup>3</sup>) of cement slurry into the hole (Melson, Rabinowitz, et al., 1979; V. F. Larson, personal communication, 1976; M. E. Stilwell, personal communication, 1976). The drill string was then pulled from the hole to replace the bit, and the section was cleaned out to a depth of 650 m sub-bottom 36 hrs. later, using a standard coring bit and core barrel. Three observations suggest that this cement probably did not drastically affect the rock in the bottom of the hole: (1) When the hole was cleaned out after cementation, hard resistance (requiring drilling) was encountered only in the 8 m between 609 and 617 m sub-bottom. (2) When the core barrel was retrieved after the cleaning operation it contained about 5 m of cuttings, but no cement. This implies that no cement ended up in the hole, since even a poorly hardened cement should have been retained to some degree (as shown by the ability of the core barrel to recover soft sediments as well as basement rocks). It cannot be ascertained how much of the material blocking the hole between 609 and 617 m was cement, although the presence of cuttings and the total absence of cement in the core barrel upon retrieval

suggests that the hole was blocked by rocks that had fallen in from the borehole wall. Interestingly, this is essentially the same depth at which this hole was blocked when we re-entered it during Leg 78B. (3) After this cementation and cleaning operation was complete, torquing was still extreme, and there was "no noticeable improvement in hole stability" (V. F. Larson, personal communication, 1976). So it appears that the mechanical integrity of the rock around the hole had not been significantly improved by this operation.

If, as the evidence suggests, the cement did not solidify in the hole, then where did it go? There are several possibilities: (1) too much water may have been pumped down the pipe during injection, and the cement may have been washed out of the annulus and deposited on the sea floor; (2) the cement may have settled into the bottom of the hole and solidified where, owing to the presence of washouts and large aperture fractures, it only filled the hole to some depth below the maximum depth reached during the final cleaning trip; or (3) the cement filled the hole as expected, but failed to set in 36 hrs. (perhaps because the downhole temperature was too low or the slurry was too dilute), and was washed out of the hole during the final cleaning trip. Regardless of our uncertainty as to the ultimate fate of this cement, we feel, for the reasons presented in the preceding paragraph, that the cementation operation probably had no significant effect on the formation permeability in the bottom of the hole.

#### Pore-Pressure Test

A pore-pressure test was conducted with the packer set in the hole at 180 m sub-bottom, using the technique already described. Figure 6 shows the downhole pressure record for this test. The hole was shut in at the packer for about three hrs. before the shear plug on the safety go-devil was blown. The minimum hole pressure attained during shut-in was 478.2 b. This is 1.5 b subhydrostatic, and provides us with an upper bound to the near-field pore pressure at this site. Although the decay in borehole pressure observed during this period was small, it is still within the approximately 0.1-b resolution of the pressure recorder. (All pressures during the shut-in period were measured relative to the hydrostatic baseline following shear-plug blow-through and packer deflation.)

A crude estimate of the undisturbed pore pressure at this site may be obtained by utilizing the Horner relationship. Accordingly, in Figure 7 we have plotted the shut-in pressure against  $\log [(T + \Delta t)/\Delta t]$ . Assuming that the pore pressure at this site was non-hydrostatic before drilling, then Hole 395A has been open to the ocean and freely flowing since drilling was completed in early January 1976; in this case the pumping time  $T$  can be taken as 5.2 y. A linear regression was then run on the data in Figure 7 to extrapolate to an initial pore pressure of 477.0 b, or 2.7 b subhydrostatic. In an infinite reservoir this pressure corresponds to the "far-field" pore pressure, that is, the pore pressure that exists beyond the radius of influence of the well. Given the scat-

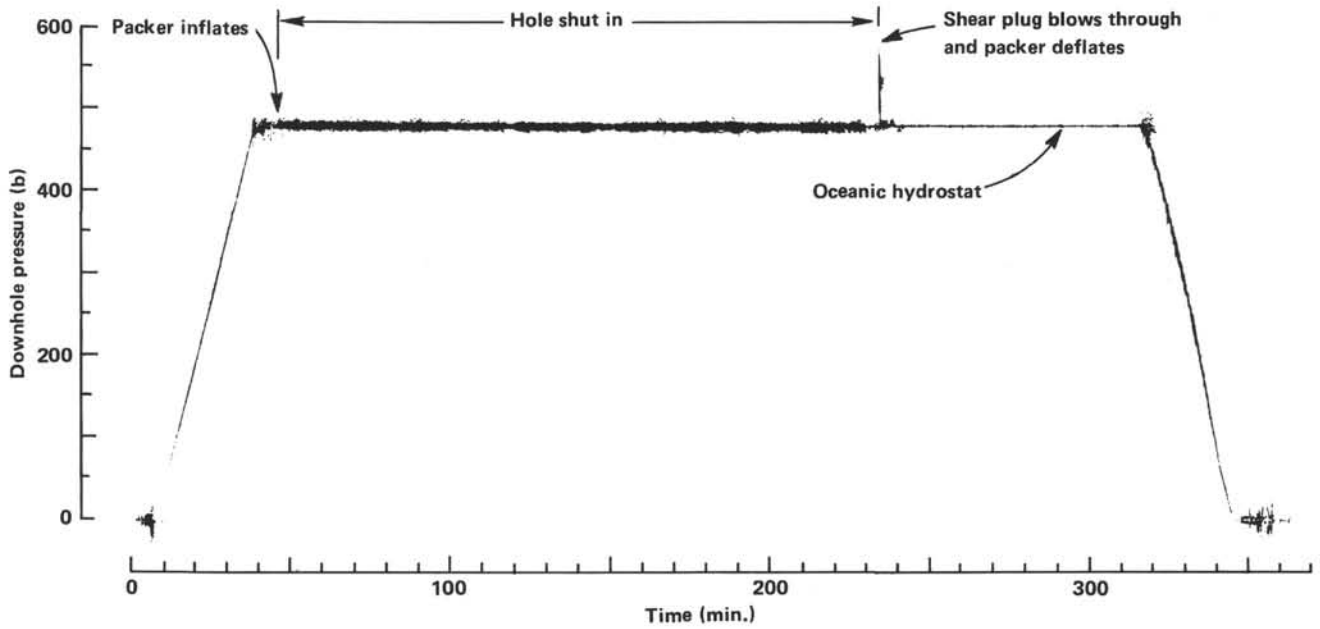


Figure 6. Downhole pressure record from the pore-pressure test conducted at 180 m sub-bottom. The sharp spike corresponds to the blowing-through of the shear plug and the subsequent deflation of the packer.

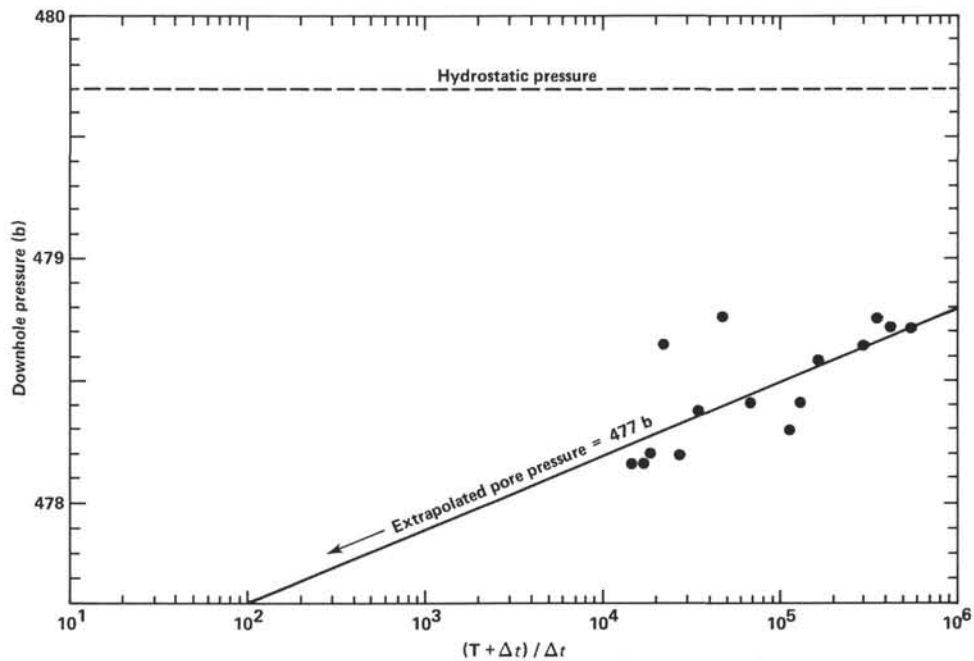


Figure 7. Data from the pore-pressure measurement at 180 m sub-bottom, plotted in accordance with the Horner method, where  $T$  is the "pumping" time and  $\Delta t$  is the time elapsed since the hole was shut in. Extrapolation is to  $\Delta t = \infty$ , that is,  $(T + \Delta t) / \Delta t = 1$ .

ter in the data, the long "pumping" time before shut-in, and the assumption of an infinite reservoir, such an extrapolation is probably of dubious validity in this case.

### DISCUSSION AND CONCLUSIONS

There are two important results from the packer tests conducted in Hole 395A. First, the bulk permeability in the basaltic breccias, pillow lavas, and dolerites pene-

trated by the deeper part of the borehole between 583 and 664 m sub-bottom at this site is very low, about  $3 \times 10^{-6}$  to  $9 \times 10^{-6}$  darcy. This is 4 to 8 orders of magnitude lower than the *in situ* permeabilities measured in basalts on land ( $3 \times 10^{-2}$  to  $3 \times 10^2$  darcies) and reported by Brace (1980), but it is well within the  $10^{-9}$ - to  $10^2$ -darcies range reported by him for *in situ* measurements in all types of crystalline rock. Second, a pore pressure



at least 1.5 b subhydrostatic was measured in the zone from 180–664 m sub-bottom, which includes the upper high permeability section.

The low-permeability zone coincides with both an increase in core recovery rate and an increase in the abundance of fractures filled with secondary minerals such as clays, zeolites, and opal below about 475 m sub-bottom (Melson, Rabinowitz, et al., 1979). Sealing of fractures and voids at depth is also indicated by the increases in borehole televiwer reflectivity (Hickman et al., this vol.), electrical resistivity, and *P*-wave velocity (Mathews et al., this vol.) observed below about 500 m sub-bottom. The failure to induce a hydraulic fracture (or, more significantly, to open pre-existing natural fractures) during our stress-measurement attempt at 583 m, even though the calculated overburden stress had been exceeded by 55 b, also testifies to the absence of weak natural fractures in the basement at the bottom of this hole. Unfortunately, owing to the failure of the permeability tests at 180 and 183 m sub-bottom in Hole 395A, we are unable to ascertain the vertical extent of this low-permeability zone; but the thermal logging results of Becker, Langseth, and Hyndman (this vol.) reveal a strongly depressed downhole temperature profile (indicating downward flow of seawater into the hole), and require both a subhydrostatic pore pressure and considerably higher permeabilities at depths shallower than the permeability test at 583 m.

The bulk permeability that we measured at the bottom of Hole 395A is 3 to 4 orders of magnitude lower than the permeabilities measured by Anderson and Zoback (1982) at shallower depths in Hole 504B near the Costa Rica Rift but comparable to the values for the lower part of that hole (Anderson et al., 1982). On the basis of the numerical model presented by Anderson and Zoback (1982), the extremely low permeability that we measured in the bottom of Hole 395A would seem to preclude significant hydrothermal convection in the ocean crust here at depths of 583 to 664 m sub-bottom. But the higher permeabilities at shallower depths, implied by the thermal logging results, together with the subhydrostatic pore pressures in this well (which might be dynamically maintained through convective processes occurring in the vicinity of the well), suggest that thermally driven circulation may be occurring at shallower depth. Vigorous circulation at shallow depths at Site 395 is also indicated by the anomalously low heat-flow values observed in the nearby sediment ponds. In a thermal model presented in this volume, Langseth et al. suggest that hydrothermal circulation directly beneath the sediment pond at Site 395 is predominantly horizontal and perhaps part of a pond-wide thermal convection cell. In contrast with the well-developed and laterally extensive sedimentary blanket at Site 504, the sedimentary blanket at Site 395 is thin and sporadic. The lack of an extensive, relatively impermeable sedimentary "lid" at this site probably greatly increases the efficiency with which heat may be convectively transferred beyond the perimeter of the sediment pond and into the water column.

If the low-permeability zone discovered at the bottom of Hole 395A is pervasive, it places strong constraints

on the vertical extent of convective hydrothermal heat transfer in young oceanic lithosphere. In this regard, preliminary analysis of more recent permeability measurements made in Hole 504B when it was re-entered and deepened during Leg 83 (Anderson et al., 1982) reveal a decrease in bulk permeability with depth of about 3 orders of magnitude, with permeability decreasing from 2–40 millidarcies at depths of 320 to 493 m sub-bottom to approximately 20 microdarcies at depths of 530 to 1280 m sub-bottom. The low permeabilities measured at the bottom of Hole 504B are thus similar in magnitude to those we measured in the bottom of Hole 395A.

The discovery of very low permeabilities at depth at Site 395, and later at Site 504, raises an interesting question: By what mechanism and at what age does this strong decrease in bulk permeability with depth occur in cooling ocean crust? Perhaps it results from some sort of "self-sealing" process whereby convection in relatively permeable, cooling ocean crust accelerates hydrothermal alteration in the host rocks and, by sealing off cracks and voids with hydrothermal alteration products, effectively shuts itself off. Further permeability and pore-pressure measurements at depth in ocean crust of varying ages should help to provide a more definitive answer.

#### ACKNOWLEDGMENTS

We would like to thank Patrick Thompson, of the Deep Sea Drilling Project, whose expertise in operating and maintaining the packer under adverse conditions was essential to the success of this experiment. We are also indebted to the rest of the staff of the Deep Sea Drilling Project and the crew of R/V *Glomar Challenger*. This manuscript was critically reviewed by Art McGarr, Larry Mastin, and Carol Morrow. This study was partially supported under NSF grant OCE 78-27026.

#### REFERENCES

- Anderson, R. N., Langseth, M. G., and Sclater, J. G., 1977. The mechanism of heat transfer through the floor of the Indian Ocean. *J. Geophys. Res.*, 82:3391–3409.
- Anderson, R. N., Newmark, R. L., and Zoback, M. D., 1982. *In situ* permeability variation in the upper kilometer of the oceanic crust of the Costa Rica Rift. *EOS, Trans. Am. Geophys. Union*, 63:434.
- Anderson, R. N., and Skilbeck, J. N., 1981. Oceanic heat flow. In Emiliani, C. (Ed.), *The Sea* (Vol. 7): New York (Interscience).
- Anderson, R. N., and Zoback, M. D., 1982. Permeability, underpressures, and convection in the oceanic crust near the Costa Rica Rift, Eastern Equatorial Pacific. *J. Geophys. Res.*, 87:2860–2868.
- Apps, J., Doe, T., et al., 1979. Geohydrological studies for nuclear waste isolation at the Hanford Reservation, Vol. II. *Lawrence Berkeley Labs Rept.* 8764.
- Brace, W. F., 1980. Permeability of crystalline and argillaceous rocks. *Int. J. Rock Mech. Min. Sci. and Geomech. Abstr.*, 17:241–251.
- Bredehoeft, J. D., and Papadopoulos, I. S., 1980. A method for determining the hydraulic properties of tight formations. *Water Resour. Res.*, 16:233–238.
- Cooper, H. H., Jr., Bredehoeft, J. D., and Papadopoulos, I. S., 1967. Response of a finite diameter well to an instantaneous charge of water. *Water Resour. Res.*, 3:267–269.
- Dmitriev, L. V., Heirtzler, J. R., et al., 1976. Drilling into ocean crust east of the Mid-Atlantic Ridge. *Geotimes*, 21:21–23.
- Engelder, T., and Scholz, C. H., 1981. Fluid flow along very smooth joints at effective pressures up to 200 megapascals. In *Mechanical Behavior of Crustal Rocks: The Handin Volume*: Washington (Am. Geophys. Union Geophys. Mono. 24), pp. 147–152.
- Horner, D. R., 1951. Pressure buildup in wells. *3rd World Petrol. Congr., Proc. Sec. II.*

- Hubbert, M. K., and Willis, D. G., 1957. Mechanics of hydraulic fracturing. *J. Petrol. Tech.*, 9:153-168.
- Hussong, D. M., Fryer, P. B., Tuthill, J. D., and Wipperman, L. K., 1979. The geological and geophysical setting near DSDP Site 395, North Atlantic Ocean. In Melson, W. G., Rabinowitz, P. E., et al., *Init. Repts. DSDP*, 45: Washington (U.S. Govt. Printing Office), 23-37.
- Kranz, R. L., Frankel, A. D., Engelder, T., and Scholz, C. H., 1979. The permeability of whole and jointed Barre granite. *Int. J. Rock Mech. Min. Sci. Geomech. Abstr.*, 16:225-234.
- Lister, C. R. B., 1972. On the thermal balance of a mid-ocean ridge. *Geophys. J. R. Astron. Soc.*, 26:515-535.
- Melson, W. G., Rabinowitz, P. D., et al., 1979. Site 395: 23°N, Mid-Atlantic Ridge. In Melson, W. G., Rabinowitz, P. D., et al., *Init. Repts. DSDP*, 45, Washington (U.S. Govt. Printing Office), 131-264.
- Papadopoulos, I. S., Bredehoeft, J. D., and Cooper, H. H., Jr., 1973. On the analysis of slug test data. *Water Resour. Res.*, 9:1087-1089.
- Parsons, B., and Sclater, J. G., 1977. An analysis of the variation of ocean floor bathymetry and heat flow with age. *J. Geophys. Res.*, 82:803-827.
- Parsons, R. W., 1966. Permeability of idealized fractured rock. *J. Soc. Petrol. Eng.*, 6:126-136.
- Purdy, G. M., et al., 1979. IPOD survey area AT-6: A site survey. In Melson, W. G., Rabinowitz, P. D., et al., *Init. Repts. DSDP*, 45: Washington (U.S. Govt. Printing Office), 39-48.
- Sclater, J. G., Crowe, J., and Anderson, R. N., 1976. On the reliability of oceanic heat flow averages. *J. Geophys. Res.*, 81:2997-3006.
- Speiss, F. N., McDonald, K. C., Atwater, T., Ballard, R., Carranza, A., et al., 1980. East Pacific Rise: hot springs and geophysical experiments. *Science*, 207:1421-1433.
- Ziegler, T. W., 1976. Determination of rock mass permeability. *U.S. Army Eng. Waterways Experiment Station Tech. Rept. S-76-2*, Vicksburg, Ms.

**Date of Initial Receipt: January 28, 1983**

**Date of Acceptance: February 22, 1983**